2011 IEEE/RSJ International Conference on
Intelligent Robots and Systems
September 25-30, 2011. San Francisco, CA, USA

Inertial Rotation Center Position Estimation for a Perching Treaded Vehicle

Christopher Schmidt-Wetekam, Nicholas Morozovsky, Thomas Bewley

***Abstract*—A method for estimating the rotation center position (RCP) of a rigid body in the x-y plane using two offset accelerometers is presented. RCP estimation via inertial measurement is motivated by the related problems of detecting foot slippage of legged robots and detecting stair edges for treaded robots, for applications in which alternative methods such as discontinuity recognition, visual tracking, and/or tactile feedback are impractical. The RCP may be directly solved for as a function of the two offset tangential acceleration measurements, when the RCP is colinear with the two accelerometers, and when the common-mode tangential accelerations, due to linear acceleration and/or gravity, can be independently measured or estimated. Angular velocity estimates may be enhanced by combining calculated angular acceleration with gyroscope measurements, even when both the RCP and common-mode tangential accelerations cannot be independently measured. An input variance modulated variable cutoff low-pass filter is also proposed for RCP estimation in the absence of independent measurements, which is validated on a balance-beam inverted-pendulum apparatus.**

I. Introduction

The combination of low-cost sensors and estimation algorithms has played a significant role in advancing the capabilities and utility of robots. For example, the dexterity of haptic manipulators has improved remarkly thanks to recent advancements in tactile sensing and high-bandwidth visual feedback [1]. Inertial sensing, however, remains an attactive strategy for mobile feedback-stabilized robots, as it is more computationally tractable using current embedded microcontrollers, and as it avoids the challenges of state estimation using vehicle-mounted cameras subject to occlusions, lighting variations, and contextual ambiguity.

MEMS-based sensors have permeated technologies such as vehicle stability control systems, motion capture [3], and video games, due to their low cost and relatively low computational overhead. Yet, even seemingly basic tasks such as localization are intractable using off-the-shelf inertial sensors alone, and significant challenges associated with shock and vibration remain. Moreover, most inertial measurement units are assumed to be nearly collocated with the rotation center position (RCP), although this restriction may be overcome on well-characterized systems when angular acceleration measurements are available [4]. When the RCP is poorly characterized, inertial RCP estimation is a desirable alternative to visual and/or tactile RCP feedback.

The authors are affiliated with the Coordinated Robotics Lab, UC San Diego, La Jolla, CA 92093-0411 USA; e-mail: cmschmid@ucsd.edu, nmorozov@ucsd.edu, bewley@ucsd.edu

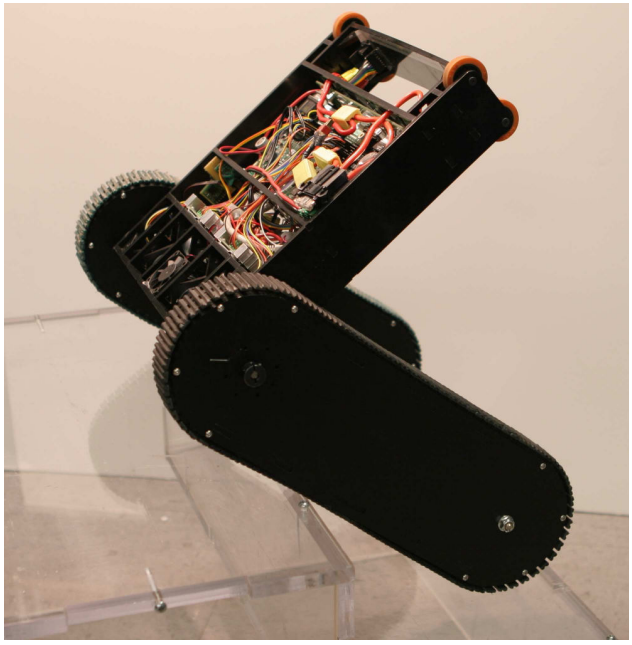

Fig. 1. Switchblade prototype in the perching configuration for climbing stairs.

This paper outlines approaches incorporating offset tangential acceleration measurements for estimating angular acceleration and velocity, common-mode acceleration, and rotation center position. The treaded-vehicle perching problem is briefly introduced, motivating an estimation approach based on a kinematic state model [5] for robust RCP estimation during transitional maneuvers. Angular velocity may be calculated directly from two offset tangential acceleration measurements, which significantly reduces angular velocity estimate high frequency noise when combined with gyroscope measurements. The common-mode acceleration variance decreases quadratically as a function of accelerometer seperation, and is minimized when both accelerometers are equidistant from the RCP, but increases with angular acceleration when the RCP is uncertain. Conversely, the sensitivity of calculated RCP variance to both measurement noise and common-mode acceleration variance decreases with angular acceleration. A first-order low-pass filter is proposed in order to refine the calculated RCP, by modulating the cutoff frequency according to the calculated RCP variance sensitivity to white measurement noise. The estimated RCP converges satisfactorily for persistently exciting angular acceleration on a balanced beam inverted-pendulum apparatus.

978-1-61284-455-8/11/$26.00 ©2011 IEEE

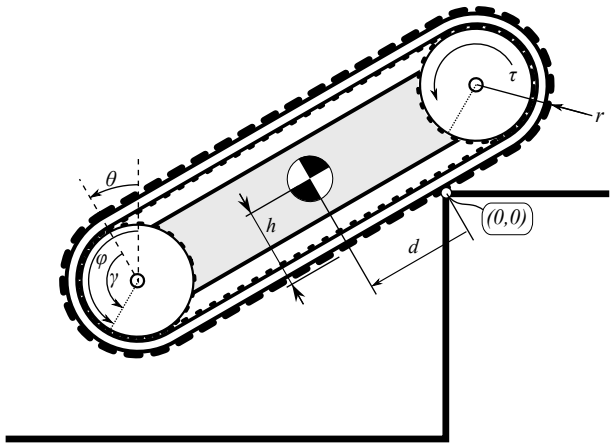

Fig. 2. Using tread actuation to restore equilibrium while perching on the edge of a step.

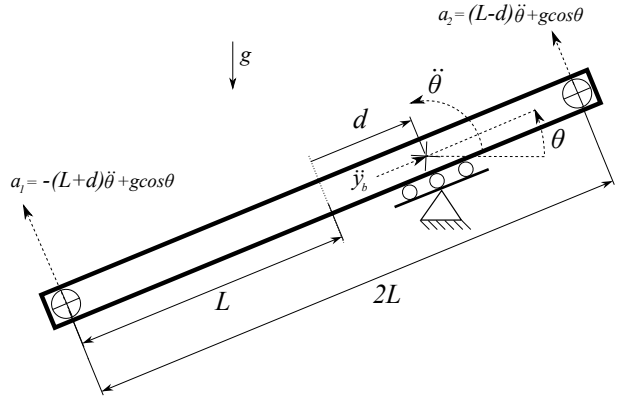

Fig. 3. Offset tangential acceleration measurements as a function of rotation center position for a perching treaded vehicle.

II. Motivation: Treaded Vehicle Perching

A treaded vehicle, dubbed "Switchblade", is part of a coordinated research program in our lab focused upon agile, compact vehicles for navigating rough terrain. One of the more advanced maneuvers under investigation is the climbing of stairs by approaching them in an upright inverted orientation, leaning the center of mass over the edge of the first step, and then driving forwards while perching on this stair edge (Fig. 2).

Using solely tread actuation, the perching dynamics are

$$E \begin{pmatrix} \ddot{\theta} \\ \ddot{\phi} \end{pmatrix} = N + \tau,$$

where

$$E = \begin{bmatrix} J + m\,(h-r)^2 + mr^2\gamma^2 & mr\,(h-r) \\ mr\,(h-r) & J_m + mr^2 \end{bmatrix},$$

$$N = \begin{pmatrix} mg\,(h-r)\sin\theta + mgr\gamma\cos\theta - mr^2\gamma\left(2\dot{\phi}\dot{\theta} - \dot{\theta}^2\right) \\ mgr\sin\theta + mr^2\gamma\dot{\theta}^2 \end{pmatrix},$$

the relative angular displacement of the tread motor shaft is

$$\gamma = \phi - \theta,$$

and the torque applied by the motors is

$$\tau = \begin{pmatrix} -su + b_m\dot{\gamma} \\ su - b_m\dot{\gamma} \end{pmatrix}.$$

When the no-slip condition holds, the position of the point of contact along the length of the tread, relative to the vehicle midpoint is

$$d = r\gamma,$$

where r denotes the radius of the tread sprocket.

The perching dynamics are most similar to the balanced-beam inverted pendulum, which may be controlled using feedback-linearized state-space control [6]. Integral action on the vehicle angle may be added in order to compensate for small positional estimate bias due to tread slippage; however, it cannot be guaranteed to converge at a rate sufficient for successfully transitioning between upright roving and perching maneuvers.

A practical means of pivot position measurement is therefore imperative for successful deployment of this particular stair climbing maneuver in the field. Pressure sensitive membrane linear potentiometers mounted beneath the treads of the current prototype provide direct edge position measurement, provided that sufficient pressure is applied at a single contact point; however, inertial edge measurement could be more robust, and would provide an added benefit of fewer additional sensors.

The tangential accelerations measured at both ends of the vehicle due to radial and angular motions (Fig. 3) are,

$$\mathbf{y} = \begin{pmatrix} a_1 \\ a_2 \end{pmatrix} = \begin{pmatrix} (h - r\gamma)\,\ddot{\theta} + {\sigma_a}^2 \\ -(h + r\gamma)\,\ddot{\theta} + {\sigma_a}^2 \end{pmatrix}, \qquad (1)$$

where ${\sigma_a}^2$ represents zero mean, white noise on both accelerometer measurements.

Denoting perturbations of the motor shaft angular displacements, γ', about a nominal displacement, γ_0, so that $\gamma = \gamma_0 + \gamma'$, the corresponding measurement perturbations, $\mathbf{y}'$, are given by

$$\mathbf{y}' = \begin{pmatrix} h - r\gamma_0 \\ -h - r\gamma_0 \end{pmatrix}\ddot{\theta}' + \begin{pmatrix} {\sigma_a}^2 \\ {\sigma_a}^2 \end{pmatrix},$$

where $\ddot{\theta}' = A(1,:)\mathbf{x}' + B_w(1,:)\mathbf{w}' + B(1,:)u'$, the state perturbations, $\mathbf{x}' = \begin{pmatrix} \dot{\theta}' & \theta' & \dot{\phi}' & \phi' \end{pmatrix}^T$, and where A, B, and B_w are the corresponding state space matrices for the state, control input, and plant disturbance perturbations, respectively.

As the perturbation in γ becomes large, the linearization must be re-evaluated, requiring some type of gain-scheduled estimation strategy. This difficulty, as well as the strong assumption that the treads will not slip, creates an incentive for an estimation approach based on a kinematic model, particularly since, in the context of perching, two offset

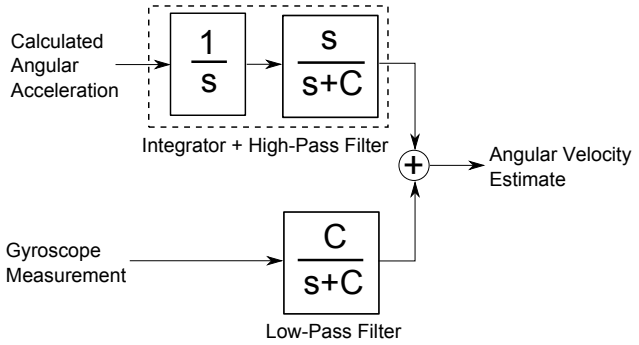

Fig. 4. Estimating angular velocity using both angular velocity and acceleration measurements.

tangential measurements, combined with an independent estimate of the acceleration due to gravity, provide sufficient information in order to solve uniquely for the RCP.

III. Angular Acceleration and Velocity Estimation

The angular acceleration may be calculated directly using offset accelerometers [2], which may be integrated in order to augment gyroscope measurements. Consider the general case of a body accelerating angularly and linearly (i.e., an unconstrained version of the configuration depicted in Fig. 3), with two sensors measuring the tangential acceleration at known distances from the center of rotation. The actual angular acceleration is related to the actual tangential accelerations by

$$\ddot{\theta} = \frac{a_2 - a_1}{2L}. \tag{2}$$

Taking into account the variance of the angular acceleration measurement noise, the variance of the calculated angular acceleration is

$$\sigma_{\ddot{\theta}}{}^2 = \frac{\sigma_a{}^2}{2L^2}, \tag{3}$$

where the accelerometer measurement noise variance, $\sigma_a{}^2$, is assumed to be zero-mean and white. Therefore, the variance decreases quadratically with increasing sensor seperation, L, so long as this added seperation does not significantly increase the component of measured acceleration due to structural modes.

Over short time horizons, angular velocity may be calculated via direct integration of the calcuated angular acceleration; however, the resulting angular velocity estimate accumulates a large bias due to amplification of low frequency noise. When gyroscope measurements are available, this bias may be bounded by combining low-pass filtered gyroscope measurements with high-pass filtered and integrated synthetic angular acceleration measurements, as depicted in Fig. 4. The resulting Power Spectral Density (PSD) of the angular velocity estimate noise asymptotically approaches the PSD of the gyroscope measurement noise at low frequencies, as the "crossover frequency", C, is raised (Fig. 5).

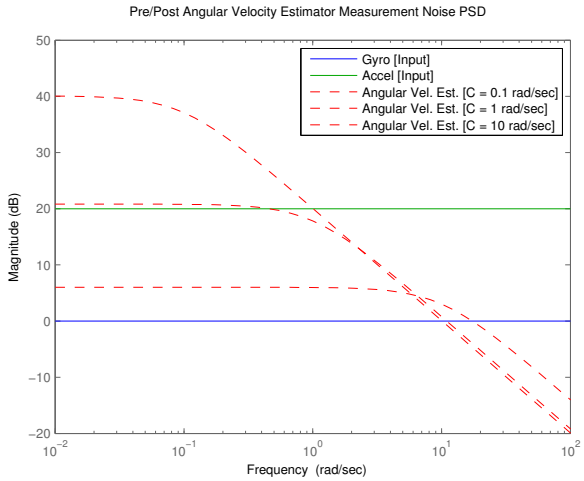

Fig. 5. Angular velocity estimate noise PSD, when measurement noise is zero mean, white with variances $\sigma_g{}^2 = 1\ rad/sec$, $\sigma_{\ddot{\theta}}{}^2 = 10\ rad/sec^2$.

The total filtered measurement noise energy over a finite frequency range of interest $[0, \Omega]$,

$$\begin{aligned} E &= \frac{1}{2\pi}\int_0^{\Omega} \sigma_g{}^2 \left|\frac{C}{j\omega + C}\right|^2 + \sigma_{\ddot{\theta}}{}^2 \left|\frac{1}{j\omega + C}\right|^2 d\omega \\ &= \frac{1}{2\pi}\int_0^{\Omega} \sigma_g{}^2 \frac{C^2}{\omega^2 + C^2} + \sigma_{\ddot{\theta}}{}^2 \frac{1}{\omega^2 + C^2} d\omega \\ &= \frac{1}{2\pi}\left(C\sigma_g{}^2 + \frac{\sigma_{\ddot{\theta}}{}^2}{C}\right) tan^{-1}\left(\Omega/C\right), \end{aligned}$$

is minimized for the crossover frequency,

$$C^* = \sqrt{\frac{\sigma_{\ddot{\theta}}{}^2}{\sigma_g{}^2}} = \frac{\sqrt{2}\sigma_a}{2L\sigma_g},$$

when $\Omega >> C$, and where the accelerometer and gyroscope noise are zero-mean and white, with variances $\sigma_g{}^2$ and $\sigma_a{}^2$, respectively.

The resulting angular velocity estimate has greatly reduced high frequency noise compared to the raw gyroscope measurement, without the significant phase loss incurred by solely low-pass filtering the gyroscope measurement (Fig. 6). Higher crossover frequencies, C, may be used in practice in order to attenuate the bias resulting from null-output accelerometer calibration error. Although generally not required for feedback control, explicit estimation of angular acceleration is a better alternative to differentiating gyroscope measurements for the purpose of linearization about a time-varying trajectory, and may also be used to boost the effective measurement range of the gyroscope, by dropping the crossover frequency towards zero as the gyroscope output saturates.

In discrete time, the low-pass filtered gyroscope measurements may be calculated using the recursion,

$$y_k = \frac{C\Delta t\left(g_k + g_{k-1}\right) - \left(C\Delta t - 2\right) y_{k-1}}{C\Delta t + 2};$$

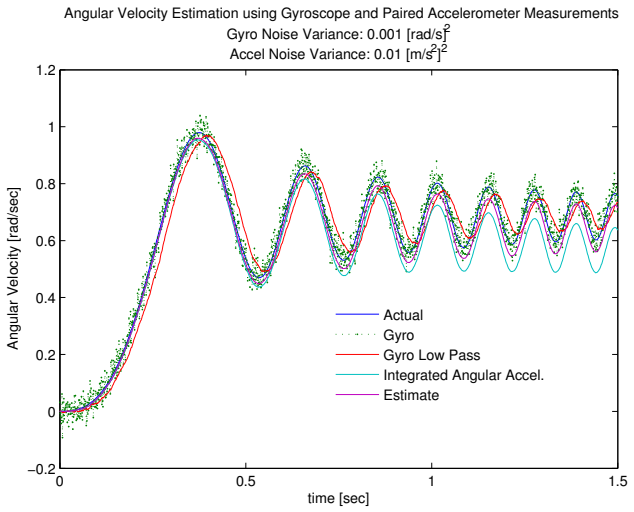

Fig. 6. Simulated angular velocity estimator response to angular acceleration chirp, for the case when accelerometer measumrent noise is biased by $+/-{\sigma_a}^2$.

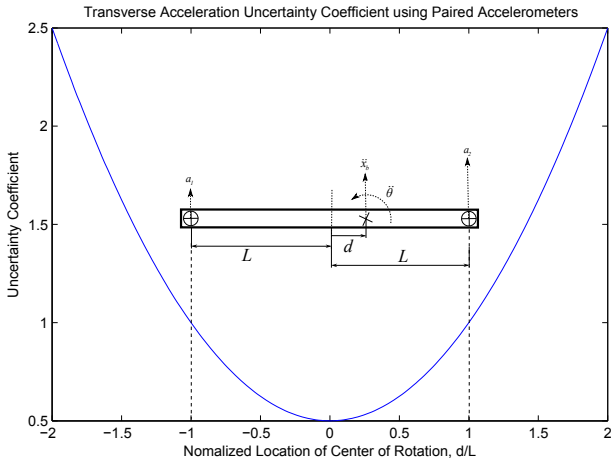

Fig. 7. The calculated transverse acceleration sensitivity to accelerometer measurement noise increases quadratically as the actual rotation axis moves away from the midpoint between the accelerometers.

similarly, the integrated and high-pass filtered angular acceleration may be calculated using

$$z_k = \frac{\Delta t\,(a_k + a_{k-1}) - (C\Delta t - 2)\,z_{k-1}}{C\Delta t + 2}.$$

The estimated angular velocity is simply

$$x_k = y_k + z_k,$$

where both y_k and z_k are computed according to the bilinear transformation shown above, where Δt is the sample time, and g_k, a_k denote the current gyroscope measurement and calculated angular acceleration (2), respectively.

IV. Common-Mode Acceleration Estimation

The actual common-mode, or transverse (body-frame), acceleration is

$$\ddot{x}_b = \frac{(L+d)a_1 + (L-d)a_2}{2L},$$

where a_1 and a_2 are the actual tangential accelerations. Taking into account the noise of the acceleration measurements,

$${\sigma_{\ddot{x}}}^2 = \frac{L^2+d^2}{2L^2}{\sigma_a}^2 + \frac{(a_1-a_2)^2}{4L^2}{\sigma_d}^2, \tag{4}$$

where σ_d denotes the uncertainty of the position of the rotation center. Note that, unlike the calculated angular acceleration uncertainty, the transverse acceleration uncertainty is not constant, as it is itself a function of the actual accelerations. The minimum common-mode acceleration variance,

$${\sigma_{\ddot{x}}}^2 = \frac{1}{2}{\sigma_a}^2,$$

when $d = 0$; i.e., the accelerometers are ideally equidistant from the center of rotation when there is no uncertainty about the location of the actual center of rotation, d (Fig.7).

Rewriting (4) in terms of the actual angular acceleration and the actual center of rotation gives

$${\sigma_{\ddot{x}}}^2 = \frac{L^2+d^2}{2L^2}{\sigma_a}^2 + \ddot{\theta}^2{\sigma_d}^2; \tag{5}$$

thus, the calculated transverse acceleration sensitivity to RCP variance increases for large angular accelerations.

A unique RCP solution exists only when the actual common-mode acceleration or actual angular acceleration can be independently determined. Denoting a_N as the tangential acceleration measured at a point colinear with a_1 and a_2, and offset a distance N from the midpoint between a_1 and a_2,

$$a_N = (N+d)\,\ddot{\theta} + X = \frac{a_1+a_2}{2} + N\ddot{\theta},$$

where X denotes the actual common-mode acceleration (in the direction of the tangential acceleration measurements). Therefore, any tangential acceleration measurement colinear with a_1 and a_2 provides no new information, as it is an offset linear combination of these two measurements.

V. RCP Estimation

In many applications, the common-mode acceleration is dominated by the component of gravity due to angular orientation, which can either be directly measured by an encoder, or estimated using an appropriately mounted IMU. In these cases, the RCP may be calculated directly using two offset accelerometers roughly colinear with the actual RCP. The actual position of the rotation center, d, is

$$d = \frac{1}{\ddot{\theta}}\left(\frac{a_1+a_2}{2} - X\right) = \frac{2L}{a_2-a_1}\left(\frac{a_1+a_2}{2} - X\right), \tag{6}$$

where a_1 and a_2 are the actual tangential accelerations, and X is the actual common-mode acceleration ($X = g\cos\theta$ for the stair-edge perching problem). Taking into account the

accelerometer measurement noise, and the uncertainty in the estimate of the common-mode acceleration,

$$\sigma_d{}^2 = \frac{1}{\ddot{\theta}^2}\left(\frac{L^2+d^2}{2L^2}\sigma_a{}^2 + \sigma_X{}^2\right), \tag{7}$$

where

$$\ddot{\theta}^2 = \frac{(a_2-a_1)^2}{4L^2} \quad \text{and} \quad \sigma_{\ddot{\theta}}{}^2 = \frac{\sigma_a{}^2}{2L^2},$$

where the accelerometer measurement noise variance is $\sigma_a{}^2$, and where $\sigma_X{}^2$ denotes the variance of estimate of the actual common-mode acceleration, X. Thus, both the variance in the calculated RCP and common-mode acceleration decrease quadratically with sensor seperation, and are minimized when both accelerometers are equidistant from the actual center of rotation. In contrast to common-mode acceleration estimation, however, the RCP variance decreases with increased angular acceleration.

In the absence of additional RCP measurements, it is proposed that the estimated rotation center, $\hat{d}$, be updated by a weighted linear combination of the previous estimate with the current calculated position:

$$\hat{d}_{k+1} = (1-A)\hat{d}_k + A\frac{2L}{a_{2k}-a_{1k}}\left(\frac{a_{1k}+a_{2k}}{2} - X_k\right), \tag{8}$$

where the normalized cutoff frequency, $A = C\Delta t$, is adjusted according to the current calculated variance (C is the cutoff frequency in rad/sec, Δt is the sample time in seconds).

The filter PSD over the finite frequency range $\omega = [0, \pi/\Delta t]$ rad/s is

$$\left|X(e^{jh\omega})\right|^2 = \frac{A^2}{2(A-1)(\cos h\omega - 1) + A^2},$$

resulting in an approximately linear relationship between normalized cutoff frequency, and white input noise attenuation (Fig. 8), so that an approximately constant variance RCP estimate is acheived via

$$A = \frac{3\sigma_E{}^2}{2\sigma_d{}^2}, \tag{9}$$

where $\sigma_E{}^2$ is the desired output variance, and when d is in fact zero mean.

As the actual variance is not constant, the calculated variance becomes highly uncertain in the absence of persistently exciting input measurements. When an upper and lower bound can be set on d (for instance, if the system has other physical constraints which limit the possible range of d), we may eliminate the dependence of (7) on d. Assuming that the center of rotation always lies between the two accelerometers, we may conservatively assume that $d = \pm L$, so that

$$\sigma_d{}^2 \approx V = \frac{1}{\ddot{\theta}^2}\left(\sigma_a{}^2 + \sigma_X{}^2\right),$$

in which case, the uncertainty of V, (that is, the approximate uncertainty of σ_d) is

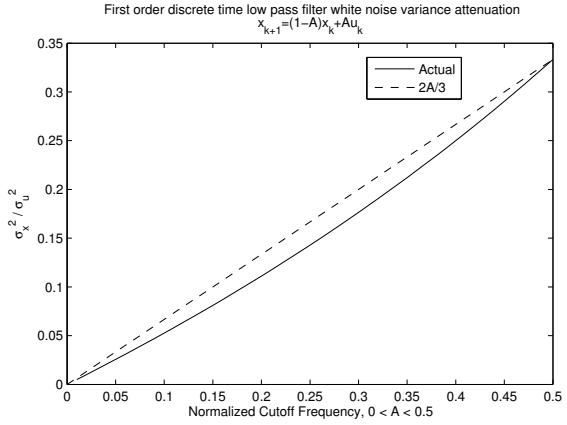

Fig. 8. Discrete time low pass filter attenuation of zero mean, white noise input, as a function of normalized cutoff frequency, A.

$$\sigma_V{}^2 = \frac{1}{\ddot{\theta}^6}\frac{2\left(\sigma_a{}^2+\sigma_X{}^2\right)^2}{L^2}\sigma_a{}^2;$$

that is, the calculated variance is itself highly sensitive to measurement noise for small angular accelerations. In order to prevent the inclusion of outliers into the estimate we may conservatively assume the worst-case variance,

$$\sigma_d{}^2 = \frac{1}{\ddot{\theta}^2}\left(\left(\frac{L^2+d^2}{2L^2} + \frac{2\left(\sigma_a{}^2+\sigma_X{}^2\right)^2}{L^2\ddot{\theta}^4}\right)\sigma_a{}^2 + \sigma_X{}^2\right). \tag{10}$$

VI. Experimental Results

The algorithm outlined by (8), (9), and (10), with $\sigma_E = 0.06$ m, produced promising results when implented on a balanced-beam inverted-pendulum (Fig. 10). As expected, the calculated RCP variance was large for small angular excitation, and vice-versa. The estimation algorithm appears to reject most outliers, yet converges rapidly with increased angular excitation. At the highest levels of angular excitation (towards the end of the data set), the estimate variance actually degrades, likely due to excitation of unmodeled structural modes.

The beam balancing apparatus used in this experiment consists primarily of a motorized linear bearing attached to a nominally horizontal beam with a central pivot (Fig. 9). Two $\pm 1.5g$ Analog Devices ADXL203 accelerometers are fitted to the linear bearing, spaced $0.5m$ apart. Each sensor exhibited a stationary measurement variance of $\sigma_a = 0.15\ m/s^2$ using a National Instuments 9201 ADC (12 Bits, $\pm 10V$). The linear bearing diplacement w.r.t. the beam fulcrum was directly measured by a rotary encoder attached to a motorized pulley. The plotted data was logged at 100Hz, during which both the linear bearing position and beam angle were controlled by hand.

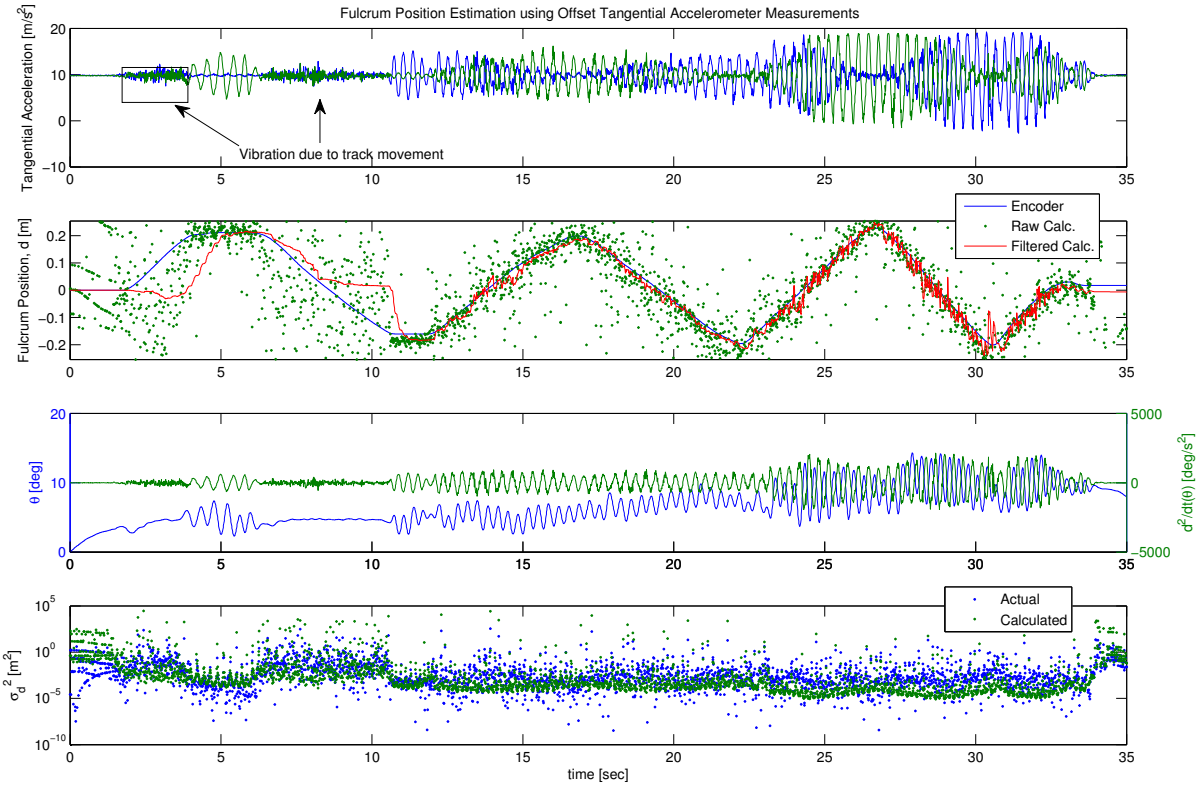

Fig. 10. Data collected using the apparatus shown in Fig. 9. The second plot is a comparison of the actual rotation center position (RCP), measured using an encoder, with the inertially-determined center of rotation (pre-filtered and post-filtered). The high uncertainty in the inertially-determined RCP (and thus slow convergence of the post-filtered estimate) occurs at low levels of angular excitation (third plot).

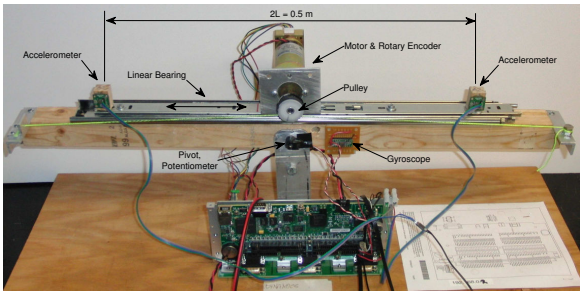

Fig. 9. Experimental apparatus for validating rotation center estimation.

VII. Conclusion

A method for estimating the planar rotation center position of a rigid body using two offset accelerometers has been developed. The RCP may be directly solved for as a function of the two offset tangential acceleration measurements when the RCP is colinear with the two accelerometers and when the common-mode tangential accelerations, due to linear acceleration and/or gravity, can be independently measured or estimated. The RCP uncertainty fluctuates significantly, as its sensitivity to accelerometer measurement noise is inversely proportional to the actual angular acceleration. The RCP uncertainty is least sensitive to measurement noise when the accelerometers are widely spaced and equidistant from the actual RCP.

Future work will focus upon implementing the RCP estimator on the current treaded robot prototype, which has already demonstrated the capability of perching using properly initialized wheel encoder measurements (attached video). Implementation on a single legged hopping robot for the purpose of detecting foot slip will also be investigated.

References

[1] Namiki, A.; Komuro, T.; Ishikawa, M.; , "High-speed sensory-motor fusion based on dynamics matching," Proceedings of the IEEE , vol.90, no.7, pp. 1178- 1187, Jul 2002

[2] Parsa, K.; Lasky, T.A.; Ravani, B.; , "Design and Implementation of a Mechatronic, All-Accelerometer Inertial Measurement Unit," Mechatronics, IEEE/ASME Transactions on , vol.12, no.6, pp.640-650, Dec. 2007

[3] Jihong Lee; Insoo Ha; , "Sensor fusion and calibration for motion captures using accelerometers," Robotics and Automation, 1999. Proceedings. 1999 IEEE International Conference on , vol.3, no., pp.1954-1959 vol.3, 1999

[4] Jau-Ching Lu; Chia-Hung Tsai; Pei-Chun Lin; , "Realization of a 9-axis inertial measurement unit toward robotic applications," SICE Annual Conference 2010, Proceedings of , vol., no., pp.2339-2344, 18-21 Aug. 2010

[5] Soo Jeon; , "State estimation based on kinematic models considering characteristics of sensors," American Control Conference (ACC), 2010 , vol., no., pp.640-645, June 30 2010-July 2 2010

[6] Chanchareon, R.; Sangveraphunsiri, V.; Chantranuwathana, S.; , "Tracking Control of an Inverted Pendulum Using Computed Feedback Linearization Technique," Robotics, Automation and Mechatronics, 2006 IEEE Conference on , vol., no., pp.1-6, Dec. 2006